

Blood Pressure Estimation Using Features Extracted from Carotid Dual-Diameter Waveforms

Prashanth Ramakrishna, Nabeel P.M, *Member, IEEE*, Raj Kiran V, Jayaraj Joseph, and Mohanasankar Sivaprakasam

Abstract— One of the major challenges in deep learning approaches to blood pressure estimation is selecting blood pulse pressure waveform features for data collection. This paper performs an analysis of a novel dataset consisting of 72 dual diameter waveform features and four blood pressure parameters. In particular, the analysis uses gradient boosting and graph theoretic algorithms to determine (1) features with high predictive power and (2) potential to be pruned. Identifying such features and understanding their physiological significance is important for building blood pressure estimation models using machine learning that are robust across diverse clinical environments and patient sets.

Clinical Relevance— Refining feature sets of physiologically relevant signals for machine learning techniques that produce cuffless estimation of carotid blood pressure parameters.

I. INTRODUCTION

The development of clinically viable, non-invasive, cuff-less blood pressure measurement technology has been notoriously elusive. However, various vectors, old and new, related to this problem are now interacting to produce cause for optimism. These vectors include but are not limited to the following: an ever-growing understanding of blood pressure's clinical significance; an exploding potential for applications to wearables such as watches, and personal healthcare monitors [3]; and a newfound technological feasibility that is the culmination of a two-decade surge in cuff-less blood pressure measurement research [1]. Still, however, the current state of affairs is characterized by fundamental limitations. The customary methods of cuff-less blood pressure measurement, derived from pulse transit time estimates, pulse contour analysis, volume clamping, and applanation tonometry are operator dependent, require constant recalibration, and suffer from sub-par accuracy [1], [2]. These limitations have fueled an increasing attraction to computational techniques – the most popular of which is machine learning – for blood pressure estimation that rely on data instead of measurement technology. This approach, although promising in certain predictable ways, comes with its own unique suite of challenges that must be addressed in its own right.

Prashanth Ramakrishna is with the New York University, New York, NY 10009 USA; e-mail: pmr347@nyu.edu).

Nabeel P M and Jayaraj Joseph are with Healthcare Technology Innovation Centre, Indian Institute of Technology Madras, Chennai, India.

Raj Kiran V is with the Department of Electrical Engineering, Indian Institute of Technology Madras, Chennai, India.

Mohanasankar Sivaprakasam is with the Department of Electrical Engineering and the Director of Healthcare Technology Innovation Centre, Indian Institute of Technology Madras, Chennai, India.

Chief among these challenges is determining what data should be used as input to whichever computational model is later constructed, and, further, how that data should be collected. Thus far, most approaches have defined their data as quantified features of the physiological blood pulse waveform, obtained from a single extremity arterial site (example: fingertip) via either photoplethysmogram (PPG) or a combination of PPG and electrocardiogram. The concerning factor, though, is that the PPG relies on blood volume fluctuations in the microvascular tissue bed, which may not be directly related to arterial pressure level [1], [7]. As a result, whatever features are extracted using this methodology may also lack sufficient relation to blood pressure, compromising the integrity of the estimations that follow. An alternative approach to obtaining waveform features in which features are extracted from physiological signals that are directly related to arterial pressure is yet to emerge for ubiquitous use.

Acknowledging the nonlinear relationship, modulated by vessel elasticity, between arterial diameter and transmural pressure, Nabeel et al. recognized the morphology of the diameter waveform as a direct representative of the bi-directionally propagating pressure wave trains. Consequently, a custom image-free ultrasound system was used for localized measurement of diameter waveforms from two proximal locations. A set of approximately 70 features, the most comprehensive gathered to date, was then derived from the dual-diameter waveforms. These features corresponded to four blood pressure reference parameters acquired from the same arterial segment using a clinical-grade tonometer synchronized with dual-diameter measurement. This approach and the resulting feature set is promising for machine learning blood pressure estimation models [8].

This paper continues of the work of [8] by performing an analysis of the aforementioned feature set using gradient boosting and graph theoretic algorithms in order to determine not only which features have the greatest predictive power, but also which features are candidates for pruning. Section II discusses data collection and extraction of the feature set. Section III discusses feature analysis. Section IV discusses the validation of the feature analysis using an artificial neural network (ANN). Finally, section V contains a summary of the paper's conclusions as well as a brief discussion.

II. DATA COLLECTION

A. Signal Acquisition

The dual-diameter waveforms were captured from two locations spaced 35 mm apart at the left common carotid site using a high frame-rate, image-free ultrasound technology,

employing a custom dual-channel probe. A calibrated tonometer sensor incorporated into the same measurement probe recorded the reference blood pressure parameters – mean arterial pressure (MAP), systolic blood pressure (SBP), diastolic blood pressure (DBP), and pulse pressure (PP) – from the carotid artery. The full hardware description is discussed elsewhere in detail [8]. However, two key points regarding the signal acquisition should be noted. Firstly, the instrumentation unit measured arterial diameter at a frame rate of 1 kHz, a virtually continuous temporal resolution, enabling reliable feature extraction. Secondly, the reference pressure waveform signal captured by the tonometer was synchronously acquired, beat-by-beat, with the dual-diameter waveform with the help of a digitally controlled a trigger pulse.

B. Feature Extraction

Signal acquisition, processing, and subsequent feature extraction were all accomplished using software developed on National Instruments' LabVIEW 2015. Isolation of cardiac cycles was automated, as was feature and blood pressure parameter extraction from each cycle. The entire feature set is detailed in Table I. Features are categorized roughly into six groups, also indicated in Table I, that, when taken together, are sufficient to quantify the pressure in the artery. At the time of their selection, however, features were chosen to comprehensively describe transmural pressure, pulse propagation speed (related to arterial elasticity) and reflection intensity [8].

III. FEATURE ANALYSIS

A. Feature Ranking

Although the chosen features intuitively bear on blood pressure due to their prominence in characterizing the diameter waveform, pulse wave velocity, or reflection intensity, it is unclear how different features contribute to the predictive power of machine learning. A first order investigation of the relative contribution of each feature to accurate blood pressure estimation was conducted using leaf-wise decision tree gradient boosting. By averaging relative feature importance over all tree expansions in the gradient boosting forest, we obtain the general relative importance of each feature. That is, if the relative importance of feature l for a single decision tree T is given by

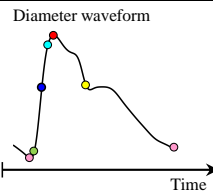
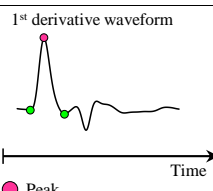
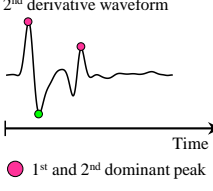
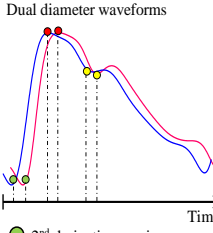
$$J_l^2(T) = \sum_{t=1}^{J-1} \hat{t}_t^2 I(v(t) = l), \quad (1)$$

where importance is measured by summing over $J - 1$ internal nodes the maximal estimated squared error risk, \hat{t}_t^2 , achieved for each partition in which variable $X_{v(t)=l}$ was chosen, then, more robustly, the relevance of feature l is taken as

$$J_l = \sqrt{\frac{1}{M} \sum_{m=1}^M J_l^2(T_m)}, \quad (2)$$

where M represents forest size. The largest value was assigned 1 and all others scaled accordingly. This feature ranking was conducted using each of the four blood pressure parameters as target outputs. It was also possible, using this technique, to determine which features do not contribute to a cumulative feature importance of 0.99 for each target output. The five most important features and the insignificant features for each blood pressure parameter are depicted in Table II [4].

TABLE I. WAVEFORM ILLUSTRATION AND EXTRACTED FEATURES

Waveforms	*a	Feature Nos.			Feature Name
		Pro	Dis	Pro-Dis	
 <p>Foot 2nd derivative maxima 1st derivative maxima Shoulder point Peak systolic Dicrotic notch</p>		F1	F35		ED to PS time
		F2	F36		Systolic 'ΔD'
		F3	F37		'D' ascend slope
		F19	F53		'D' ascend area
		F4	F38		PS to ED time
		F5	F39		Diastolic 'ΔD'
		F6	F40		'D' descend slope
		F20	F54		'D' descend area
		F25	F59		Systolic area
		F26	F60		Diastolic area
		F27	F61		Shoulder point to PS slope
		F28	F62		Dicrotic notch to ED slope
		F29	F63		ED diameter
		F30	F64		Peak distension
 <p>Peak 1st and 2nd Valley</p>		F31	F65		Distensibility
		F32	F66		Shoulder point to PS time
		F33	F67		Dicrotic notch to ED time
		F34	F68		Total cycle time
		F7	F41		Valley1 to Peak time
		F8	F42		Ascend intensity
		F9	F43		Ascend slope
		F10	F44		Peak to Valley2 time
		F11	F45		Descend intensity
		F12	F46		Descend slope
 <p>1st and 2nd dominant peak Valley</p>		F21	F55		Ascend area
		F22	F56		Descend area
		F13	F47		Valley1 to Peak time
		F14	F48		Ascend intensity
		F15	F49		Ascend slope
		F16	F50		Peak to Valley2 time
		F17	F51		Descend intensity
		F18	F60		Descend slope
 <p>2nd derivative maxima Peak systolic Dicrotic notch</p>		F23	F57		Ascend area
		F24	F58		Descend area
			F69		PTT at 2 nd derivative max
			F70		PTT at PS
			F71		PTT at dicrotic notch

PS: Peak systolic, ED: End diastolic, D: Diameter, ΔD: Change in diameter, Pro: Proximal and Dis: Distal, *a: Group color coding

Instantaneous pressure change features are directly related to blood dynamics (flow, in particular) and have therefore been ubiquitously used in machine learning approaches to blood pressure estimation. It should be noted that, as shown in Fig. 1, the feature group the accounts for the most cumulative relative importance is instantaneous pressure changes. The ubiquitous use of the features contained therein is therefore justified. However, excluding the other feature groups, which

TABLE II. MOST IMPORTANT FEATURES BY PARAMETER

Relevance	MAP	SBP	DBP	PP
Important	F27, F13, F3, F53, F54	F25, F63, F8, F12, F56	F14, F27, F22, F29, F21	F25, F63, F8, F21, F22
Insignificant	F30, F31, F64, F65, F68	F1, F30, F64, F65	F30, F31, F64, F65, F70	F30, F31, F64, F65, F66

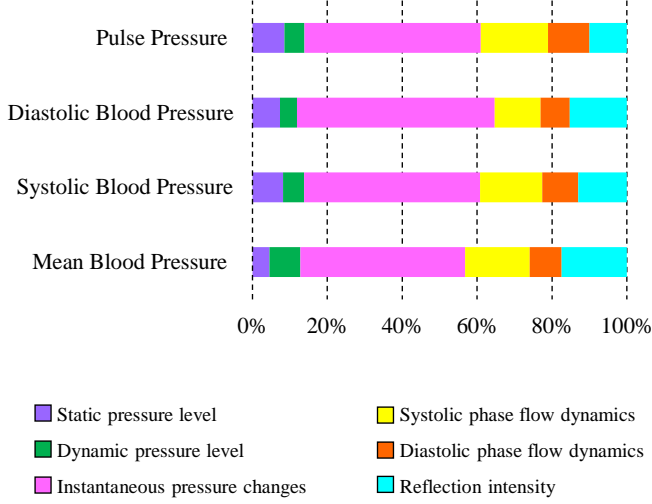


Figure 1. Cumulative feature group importance for each blood pressure parameter.

account for over 50% of relative cumulative importance is not recommended.

Interestingly, end diastolic diameter (F63, F29), appears as an important feature not only for diastolic pressure, of which it is a direct representation, but also for systolic pressure. Because diastolic and systolic pressure vary proportionally, except in cases of isolated hypo- or hyper-tension, end diastolic diameter is acting, here, as a surrogate for both diastolic and systolic pressure. This is consistent with the character of the patient set from which the dataset was acquired, in which no instances of isolated isolated hypo- or hyper-tension were included.

Finally, at least one feature representing reflection intensity group was expected to contribute significantly to systolic pressure estimation. However, data limitations in the age diversity of the patient set, which is entirely young, resulted in waveforms that lacked strong arterial wave-reflections that affect the systolic phase.

A. Meta-Features

Analysis of the structure of correlations between various features was also undertaken to extract “meta-features”, that is exclusive groups of highly colinear features that, when taken together, represent the same waveform characteristics. This was done by transforming the features correlation coefficient matrix into an adjacency matrix where correlations > 0.95 were set to 1 and those < 0.95 were set to 0. From the graph described by the adjacency matrix – plotted as a schema ball in Fig. 2 – we identified and extracted all cliques using a modified K -clique finding algorithm. Given an undirected graph $G = (V, E)$, where V is the set of the graph’s vertices and E the set

TABLE III. META-FEATURE CLIQUES

Clique Size	Clique			
2	F55, F21		F14, F15	
3	F17, F18, F24	F64, F65, F36	F30, F31, F2	F51, F52, F58

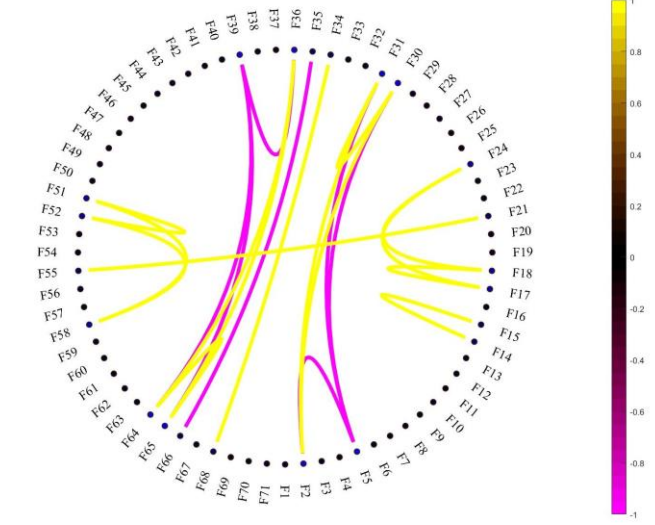


Figure 2. Correlation coefficient matrix represented as a schema ball (only absolute correlations greater than 0.95 are shown)

of its edges, a clique is a collection of vertices $C \subseteq V$ such that the subgraph S induced by C is complete. By convention, $|C| = K$. The members of the identified cliques are listed in Table III. Note that these cliques validate the qualitative feature groupings defined in Fig. 1.

They also align with the features identified as commonly insignificant in Table II for each blood pressure parameter. Pairs F30 and F31, as well as F64 and F65 belong to the same clique. Because the members of these cliques are highly colinear exclusively with each other, two of the three members may contribute minimally to the learning process and only one will be retained. For the purposes of this paper, only those features that did not contribute to a cumulative feature importance of 0.99 are included in Table II. However, F14, F24, and F58 all appear in the top ten most insignificant features with importances < 0.008 . The question of why the additional three features one would expect to be extremely insignificant are not is an interesting one, whose answer is likely found in the many correlational dependencies not shown in Figure 2.

Clique (F17-F18-F24) describes the proximal wave’s upstroke intensity; clique (F51-F52-F58) describes the distal wave’s upstroke intensity; clique (F30-F31-F2) describes the arterial distensibility experienced by the proximal wave; clique (F64-F65-F36) describes the arterial distensibility experienced by the distal wave; and, finally, clique (F55-F21) describes arterial hyper-elasticity. It is unclear whether clique (F14-F15) does indeed describe a meta-feature. These five meta-features presents further opportunity for pruning the feature set, since only a single feature is necessary to describe each one.

TABLE IV. MEAN ABSOLUTE ERROR WITH AND WITHOUT INSIGNIFICANT FEATURES

Trial	Mean Absolute Error (mmHg)			
	MAP	SBP	DBP	PP
Original Feature Set	6.432	15.982	11.140	6.492
Pruned Feature Set	6.710	8.094	5.496	7.701

One interesting observation was the almost 4-clique (F33-F68, F33-F34, F34-F4, F34-F68, F68-F4), which again highlighted the patient set's lack of age diversity. All the features in the clique are directly proportional to heart rate. For this reason, they are also proportional to each other. However, if the patient set were more diverse in age and, more specifically, diverse in vascular age, then F33, the time from the dicrotic notch to the end of the diastolic phase would not necessarily be directly proportional to heart rate.

IV. MACHINE LEARNING VALIDATION

A. Artificial Neural Network Architecture

For validation of the previously discussed feature analysis, a feed forward artificial neural network was used. The machine learning model was implemented using Keras, powered by a TensorFlow engine, on Python 3.7. The network's architecture consisted of 71 input neurons, a single output neuron, and four fully connected or "dense" hidden layers of sizes 70, 70, 40, and 10 respectively. That is, letting $w_{ij}^{(k)}$ be the weight corresponding to the connection between the i^{th} neuron in layer k and the j^{th} neuron in layer $k + 1$, the output of the j^{th} neuron in layer $k + 1$ can be expressed as

$$n_{(k+1)j} = \sigma \left(\sum_i w_{ij}^{(k)} n_{ki} \right) \quad (3)$$

where σ is the non-linear activation function. Here, ReLU was chosen as the activation function. After each forward pass, the loss is calculated as mean squared error and the network's weights are updated accordingly using stochastic gradient descent.

B. Evaluation with and without Low-Importance Features

The ANN described above was used to estimate the four blood pressure parameters first with the entire original feature set and second with a pruned feature set. The pruned feature set excluded those features identified as insignificant using gradient boosting. The mean absolute error achieved after training on randomly chosen test data is displayed in Table IV.

Notice that post-pruning, the ANN performed significantly better in estimating systolic and diastolic pressure, improving by approximately 50% on both fronts. This is likely due to overfitting with respect to the insignificant features when learning on the original feature set. More broadly, these results provide a validation of machine learning using a comprehensive dual diameter waveform feature set in order to determine blood pressure, since the absolute errors achieved are less than the usual error of 9 mmHg of non-computational, indirect methods of blood pressure measurement.

V. CONCLUSIONS AND FUTURE RESEARCH DIRECTIONS

In this paper a comprehensive dual diameter waveform feature set, used by machine learning to estimate blood pressure, was explored in order to gain insight into the physiological significance of various features and to discover opportunities for pruning. Pruning is beneficial not only because it decreases the time and effort required in data gathering, but also because it decreases computational load during learning. Gradient boosting was used to identify insignificant features and a graph theoretic approach to analyzing feature correlations was used to uncover physiologically significant waveform meta-features such as upstroke intensity and arterial distensibility. Finally, an ANN was used to evaluate estimation of four blood pressure parameters using both a full and pruned feature set.

There are, however, certain limitations of this work that must be noted. Firstly, and most importantly, the limitation of age diversity in the patient set from which the data were drawn must be acknowledged. Generation of data from more diverse patient set is in progress. This is necessary in order to properly assess which features have predictive power across general populations. Data would also be generated based on BP intervention methods, applicable at individual level. Secondly, while computational analyses can be powerful, drawing meaning from their results can be a dubious enterprise. In this study, physiological significance was only noted when it was most obvious. However, the mere existence of a highly colinear clique, for example, doesn't necessitate its representation of a meta-feature. Thirdly and finally, validation of a pruned feature set that was pruned based on identified meta-features was not done. This was because an adequate method of removing members of a meta-feature clique while retaining the information they provide via other potentially significant correlational relationships was lacking and efforts in this direction are underway. Future work in total focuses on addressing all three of these limitations.

REFERENCES

- [1] R. Mukkamala et al., "Toward ubiquitous blood pressure monitoring via pulse transit time: theory and practice," *IEEE Trans. Biomed. Eng.*, vol. 62, no. 8, pp. 1879–1901, 2015.
- [2] X. R. Ding et al., "Continuous blood pressure measurement from invasive to unobtrusive: celebration of 200th birth anniversary of carl ludwig," *IEEE J. Biomed. Heal. Informatics*, vol. 20, no. 6, pp. 1455–1465, 2016.
- [3] A. Stojanova et al., "Continuous blood pressure monitoring as a basis for ambient assisted living (AAL) – review of methodologies and devices," *J. Med. Syst.*, vol. 43, no. 24, pp. 1–12, 2019.
- [4] T. Hastie, R. Tibshirani, J. Friedman, *The Elements of Statistical Learning: Data Mining, Inference, and Prediction*. New York: Springer-Verlag, 2004, ch. 10.
- [5] E. Chung et al., "Non-invasive continuous blood pressure monitoring : a review of current applications," *Front. Med.*, vol. 7, no. 1, pp. 91–101, 2013.
- [6] J. Xia et al., "Pulse wave analysis for cardiovascular disease diagnosis," *Digit. Med.*, vol. 4, no. 1, pp. 35–45, 2018.
- [7] S. G. Khalid et al., "Blood pressure estimation using photoplethysmography only : comparison between different machine learning approaches," *J. Healthc. Eng.*, vol. 2018, no. 1548647, pp. 1–13, 2018.
- [8] N. P. M. et al., "Deep Learning for Blood Pressure Estimation: an Approach using Local Measure of Arterial Dual Diameter Waveforms," *Australas. Phys. Eng. Sci. Med.*, vol. 37, no. 2, pp. 367–376, 2019.